Indonesian Journal of Aerospace Vol. 21 No. 2 December 2023 : pp 121 – 132 (Herdiana et al.)
DOI: 10.55981/ijoa.2023.1050
https://ejournal.brin.go.id/ijoa/

Parachute Design and Wind Tunnel Testing of Class 10 kg LAPAN UAV Recovery System

Dana Herdiana[1], Teuku M. Ichwanul Hakim[2], Ardanto M. Pramutadi[3], and Waryoto[4]

1PRTP, National Research and Innovation Agency-BRIN, Indonesia
2PRTP, National Research and Innovation Agency-BRIN, Indonesia
3PRTP, National Research and Innovation Agency-BRIN, Indonesia
4DPLFRKST,NationalResearchandInnovationAgency-BRIN,Indonesia
e-mail:dana006@brin.go.id,teuk003@brin.go.id,arda001@brin.go.id,andwary001@brin.go.id

Received: 08-02-2023 Accepted: 30-10-2023 Publishied: 31-12-2023

Abstract

LAPAN (BRIN) has already developed several types of fixed-wing UAVs that are intended to conduct civil applications. The UAV is divided by a weight class, which is 10 kg, 20 kg, and 30 kg in MTOW. In some missions, the UAV can operate in the normal way, take-off and landing by using a small runway. In some other missions, the UAV has to be launched by using a catapult and landing by net because of limited space. In the case where the UAV has to be landed between the trees, the usage of nets is not possible. Therefore the recovery system by using a parachute is designed. The cross-type parachute is designed by using analytical and simulation methods to calculate the descent velocity when the aircraft vertically lands. The descent velocity is derived from structure and payload requirements where the impact when the aircraft touches the ground will not cause damage. The designed parachute was then tested in a LAPAN Low-Speed Tunnel (LLST) to verify the design. The tests are conducted in various Reynolds numbers to observe parachute characteristics at a wide range of velocity. The wind tunnel model which is used in the test has a scale of 1:6. The Result of the simulation and the test shows that the design of the parachute was sufficient to be used as a recovery system for a class 10 kg LAPAN UAV because the descent velocity requirement is fulfilled.

***Keywords**: UAV, recovery system, parachute, wind tunnel.*

1. Introduction

LAPAN (BRIN) has already developed several types of fixed-wing civil UAVs. Recently, unmanned aerial vehicles (UAVs) have been employed extensively in military and civil use. In different operations, one of the biggest limitations of UAVs is the lack of autonomous aerial refueling (AAR) capability, which results in a short loiter time (Wang Xufeng, 2015). The developed UAV is divided by a weight class, which is 10 kg, 20 kg, and 30 kg in MTOW. Those UAVs are intended to support LAPAN (BRIN) to conduct missions that are related to surveillance and mapping. It is also utilized by other government institutions e.g. Indonesian Ministry of Agriculture or the Ministry of Forestry to support their mission in an area of observation and mapping. Examples of missions of LAPAN's UAV have been done e.g. observation of the active volcanoes, forest mapping, plantation, and rice field mapping, and post-disaster monitoring (flood, eruption landslide, etc.).

In many missions, the UAV Class 10 kg is often used. It is small and relatively lightweight, making it easy to carry to the mission area even though the location is difficult to access. Smaller UAVs are easiest to be operated, they can use the road as a runway for take-off and landing. The UAV Class 10 kg is shown in Figure 1-1-1.

For the missions that are prepared well, where the operator has plenty of time to arrange the flight plan, for example, rice field mapping, aerial photography, etc. The UAV can be operated in a normal way. It is take-off and landing using a small runway or normal road.

Figure 1-1. LAPAN's UAV class 10 kg. (Pustekbang LAPAN, n.d.)

In some other missions e.g. flood or landslide monitoring, where the result of monitoring shall be produced quickly, the operator has only limited time, and in most cases, the infrastructure for UAV operation is not sufficient, there should be an alternative way to operate the UAV. Then the UAVs are launched using a catapult and landing by nets because of limited available space in the mission area. The operation of LAPAN's UAV using nets is shown in Figure 1-2.

Figure 1-2. Aircraft recovery by using nets. (Pustekbang LAPAN, n.d.)

In a mission where the nets are difficult to provide, the use of the parachute as a recovery system is the option to solve the problem of landing, especially in very narrow spaces such as landing between trees. This provides insight into the drag and stability of parachutes in a low subsonic environment but cannot always be compared to the flight conditions of actual operation (L. Pepermans, 2021).

Compared to the nets, the advantages of parachute usage are easy to operate, simple, compact, and lightweight. With those advantages, therefore the design of a recovery system for the UAV using a parachute is worth it.

In the design of a recovery system using a parachute, there is some importance to know. It was set up that the forebody wake can remarkably affect the drag coefficient by changing the length of the suspense line, which can ameliorate the drag performance (Xiaopeng Xuea, 2017). The effects of the suspense lines on the performance of parachute shave have been widely investigated using experimental studies (Xiao-peng Xue, 2015). Steinberg et al. (S. Steinberg, 1974) showed that the suspense line length rate (i.e., the rate of the length of the suspense line to the diameter of the canopy) directly affects the drag coefficient of the parachute system with Mach number ranging from Mach 0.2 to2.6 (Xiao-peng Xue, 2015). In studies using wind tunnels, the flexible structure of the chute made measurements difficult (Nimesh Dahal, 2020).

Based on the problems above, it is necessary to design an appropriate parachute with simulation and test the parachute in a wind tunnel as validation. The simulation uses Computational Fluid Dynamics (CFD) based on Ansys CFX and the wind tunnel test using LAPAN/BRIN Low-Speed Tunnel. The CFD simulation results and experiments are

compared to prove that this CFD method can accurately simulate the descent velocity under the same parameter conditions as the wind tunnel test.

The objective of this study was to design a recovery system in the form of a parachute, to be applied in 10 kg of the UAV class. In this study, the cross-type parachute was selected with the consideration of descent stability. The parachute shall be able to deliver the UAV landed safely without any damage.

2. Methodology

The objective of the parachute design is to fulfill its requirements which is to land the UAV safely in any kind of operation and altitude.

In the first phase of design, parachute sizing was calculated based on the weight of the UAV and the target descent velocity. This phase will result from the required drag coefficient and total parachute size. The next step is to test the initial design by using CFD to simulate forces produced by the parachute. A wind tunnel test was done to verify the result of the simulation.

The methodology used in this study is shown in Figure 2-1.

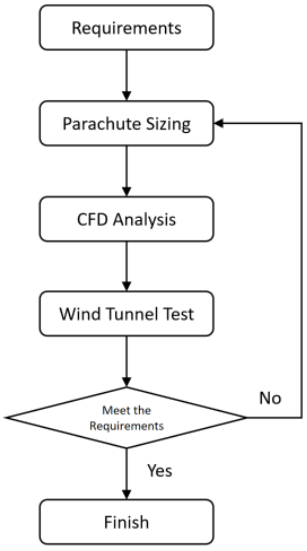

Figure 2-1. Methodology

2.1. Parachute Aerodynamic Theory

Parachute works by decelerating the descent rate of a falling object by using the principle of drag which acts opposite to the gravitation or direction of descent. The drag force of the parachute is dependent on dynamic pressure, parachute area, and parachute drag coefficient. The cross-type parachute is designed by using analytical methods to calculate the descent velocity or stable descent rate when the aircraft vertically lands. It is derived from structure and payload requirements where the impact when the aircraft touches the ground will not cause damage. In this case, the descent velocity of 2 m/s is used as the target.

The basic equation used in the design of the parachute is the drag equation:

$$\mathrm{D} = \frac{1}{2}\rho \mathrm{V}^2 \mathrm{A} \mathrm{C}_\mathrm{d} \qquad (2\text{-}1)$$

The descent velocity of a falling object is related to the object's mass, gravitational acceleration, and parachute drag.

$$\mathrm{D} = \mathrm{m} \cdot \mathrm{g} \qquad (2\text{-}2)$$

Therefore it can be written as follows (Zhibin Li, 2021):

$$m \cdot g = \frac{1}{2}\rho V^2 A C_d \qquad (2\text{-}3)$$

For the real parachute which is used as the recovery system, total drag is the sum of the drag of the parachute with the drag of the UAV. To simplify the case, in this study drag of the UAV is neglected. The required drag coefficient can be calculated using the following formula (Zhibin Li, 2021):

$$C_d = \frac{2 \cdot m \cdot g}{\rho V^2 A} \quad (2\text{-}4)$$

To obtain parachute size, it is assumed that the parachute has a similar Cd value as the hemisphere parachute which is 1.5 (NASA, n.d.) (Hoerner, 1965). With the rearranged drag equation above, the required area of the parachute can be solved:

$$\mathrm{A} = \frac{2 \cdot m \cdot g}{\rho \cdot V^2 \cdot C_d} \quad (2\text{-}5)$$

It is assumed that the canopy area will be 0.58% of the flattened area, therefore it is obtained the dimension of the flattened parachute as is shown in Figure 2-2.

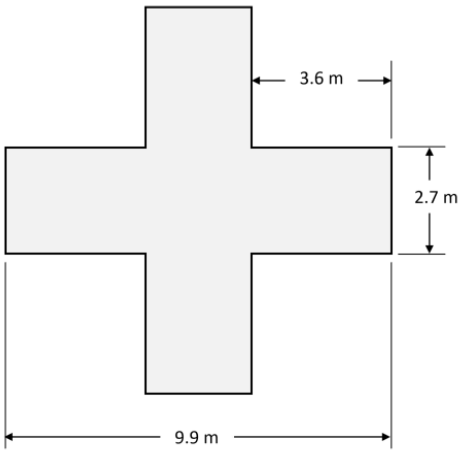

Figure 2-2. Parachute size.

2.2. CFD Analysis

For Fluid Dynamics, the airflow is assumed to be at low speeds and thus the Navier-Stokes equations of incompressible flows are utilized (Keith Stein R. B., 2001). The Navier-Stokes equations for incompressible flows are (T.E. Tezduyar, 1994):

$$\rho_f \left(\frac{\partial u}{\partial t} + u.\nabla u + f \right) - \nabla.\sigma_f = 0 \ \ on\ \Omega \quad (2\text{-}6)$$

$$\nabla.u = 0 \ \ on\ \Omega \quad (2\text{-}7)$$

Where ρ_f, u, f, and σ_f are the fluid density, velocity, body force, and stress tensor, respectively. For a fluid with dynamic viscosity μ and the strain rate tensor ε(u), the stress tensor is defined as follows:

$$\sigma_f(p,u) = -pI + 2\mu\varepsilon(u) \quad (2\text{-}8)$$

Where I is the identity tensor, p is the pressure. For the problems under consideration, μ is augmented locally using a Smargorinsky turbulence model (Smagorinsky, 1963) (Keith Stein R. B., 2001).

Fluid pressure is defined by the ideal gas state equation (Hou Xia-yi, 2022):

$$p = \rho_f(Cp - Cv)T \quad (2\text{-}9)$$

Where Cp and Cv are the specific heat capacities at constant pressure and volume respectively, T is the temperature of the fluid. The governing equation of the structure is described in the Lagrangian frame (Hou Xia-yi, 2022):

$$\rho_s \frac{d^2 v}{dt^2} = div(\sigma_s) + \rho_s f_s + g \quad (2\text{-}10)$$

Where ρ_s denotes the density of the solid, v represents the displacement of the solid structure nodes, σ_s is the Cauchy stress tensor, f_s is the body force acting on the structure, t represents the time, and g is the gravitational acceleration.

The turbulent model used in the CFD simulation is Shear Stress Transport (SST) because Shear Stress Transport uses a robust two-equation eddy-viscosity turbulence model. The model combines the k-omega turbulence model and the K-epsilon turbulence model such that the k-omega is used in the inner region of the boundary layer and switches to the k-epsilon in the free shear flow (Gamiz, 2013). So this turbulent model can calculate flow velocity conditions that are attached to the parachute surface.

2.3. Simulation Parameter

CFD simulation was done to simulate that the parachute is under test inside the wind tunnel. This method was chosen with the consideration that in the wind tunnel test, the accuracy of the test result will be influenced by its material weight, especially at very low velocity. Simulation was carried out with velocity variations 4, 5, 6, 7, 8, 9, and 10 m/s. It was done with the help of CFD code Ansys CFX solver.

Figure 2-3 shows the geometry of the numerical wind tunnel domain with a cross parachute as a test model in the center. The fluid dynamics model is developed to be representative of the wind tunnel (Keith Stein R. B., 1999). The LLST wind tunnel has a test section dimension of 2,250 mm x 1,750 mm x 10,000mm.

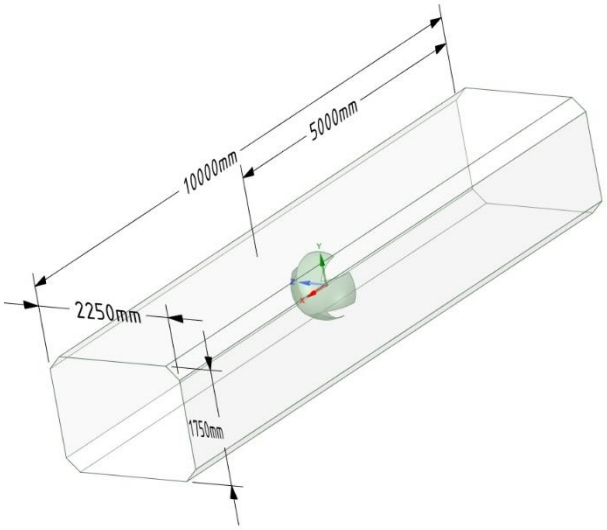

Figure 2-3. Numerical wind tunnel domain and Cross parachute model.

The boundary condition of the simulation is shown in Figure 2-4, and the parameter setup in the simulation can be seen in Table 1.

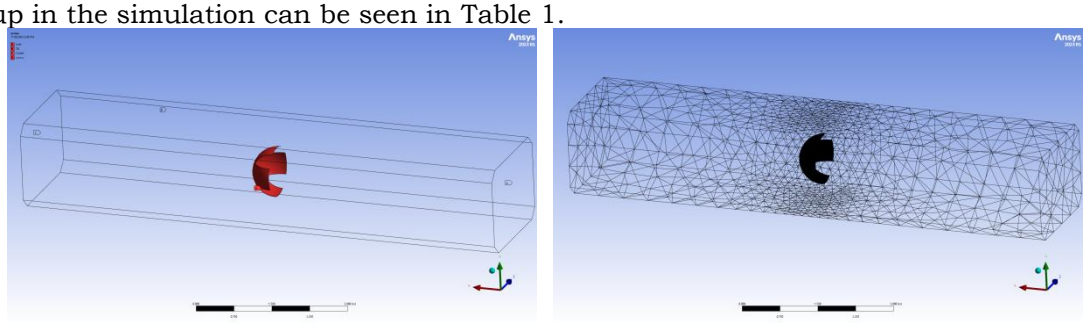

Figure 2-4. Domain of the simulation conditions (ANSYS, 2023).

Table 1. Parameter setup for simulation.

Solver	CFX
Models Turbulent	Shear Stress Transport
Material	Air ideal gas (air)
Density	1,225 kg/m^3
Viscosity	1,7894 x 10-5 kg/m-s
Operation Pressure	1 atm = 101325 N/m^2
Boundary condition Inlet	Normal speed
Boundary condition of parachute	Wall
Boundary condition Wind Tunnel	Wall
Boundary condition Outlet	Normal speed
Flow velocity	4, 5, 6, 7, 8, 9, and 10 m/s
The angle of attack (α)	0°

To find out the relationship between the number of elements (mesh) and the simulation results, a sensitivity grid/mesh is carried out by varying the number of elements see Figure 2-5.

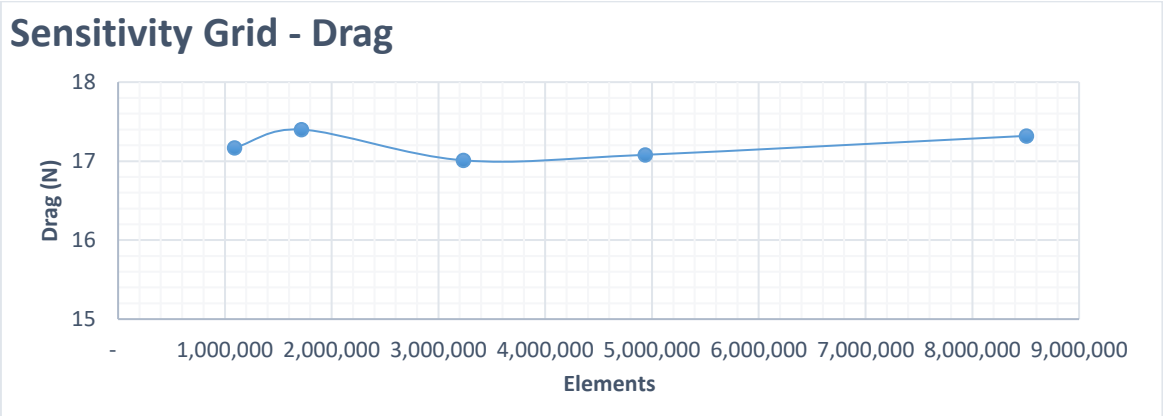

Figure 2-5. Sensitivity grid with varying number of elements.

Figure 2-5 shows the sensitivity grid levels by varying the number of elements. This sensitivity grid is carried out by assuming a velocity of 4 m/s and a coarse level is medium. Judging from the sensitivity grid graph, the resulting drag value is quite good because the value is quite stable with increasing number of elements. For this reason, the simulation was carried out with a number of elements of around 3.2 million.

2.4. Wind Tunnel Test

According to Linghard (J S. Lingard, 2017), wind tunnels have the advantage that tests can be performed in controlled environments where the operator can control parameters such as Mach number and dynamic pressure. This allows for the validation of drag performance and stability. Wind tunnels proffer the unique possibility of analyzing and observing the parachute in a way that cannot be done in flight (L. Pepermans, 2021).

To test the parachute in the wind tunnel, it has to be scaled down from the original size to fit in the test section. In addition to ensuring that the model fits in the test section, scaling down the model is also considered the wall blockage to provide measurement accuracy. The final dimension of the model is shown in Figure 2-6 and listed as follows:

- Model scale: 1:6
- Flattened diameter: 1.65 m
- Canopy diameter: 1.0 m
- Gore number: 9
- Rope length: 1.76 m

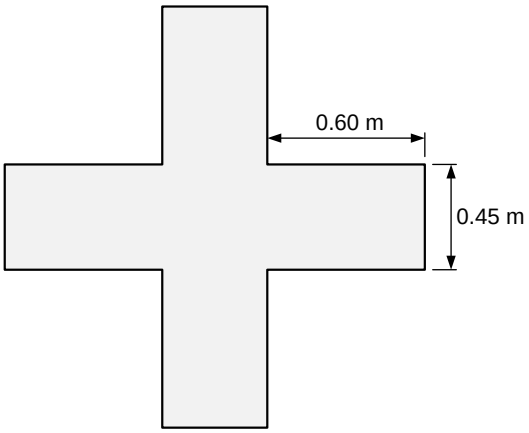

Figure 2-6. The flattened shape of the wind tunnel parachute model.

The parachute model was tested in a LAPAN low-speed tunnel (LLST) to obtain its drag coefficient (Cd) characteristic. Below are specification of the LLST:

- Wind tunnel type : open loop circuit
- Cross section area of test section : 1.75 m × 2.25 m
- Maximum speed in the test section : 60 m/s
- Speed control : automatic and manual

- Force measurement : internal and external balance

The testing was done in the velocity range from 4 m/s to 10 m/s, with a velocity increment of 1 m/s. The rope length also varied for scale 1:1 and scale 1:0.85. Force measurements were done by using an external balance with the help of strut support to transfer the force to the balance. The velocity of 4 m/s to 10 m/s was chosen because at a velocity of 4 m/s, the parachute had started to expand or form a canopy cross so test data could not be obtained for the target velocity of 2 m/s. Figure 2-7 shows the drawing of the test facility LLST. The schematic of the model installation in the wind tunnel is shown in 2-8 and parachute testing is shown in 2-9.

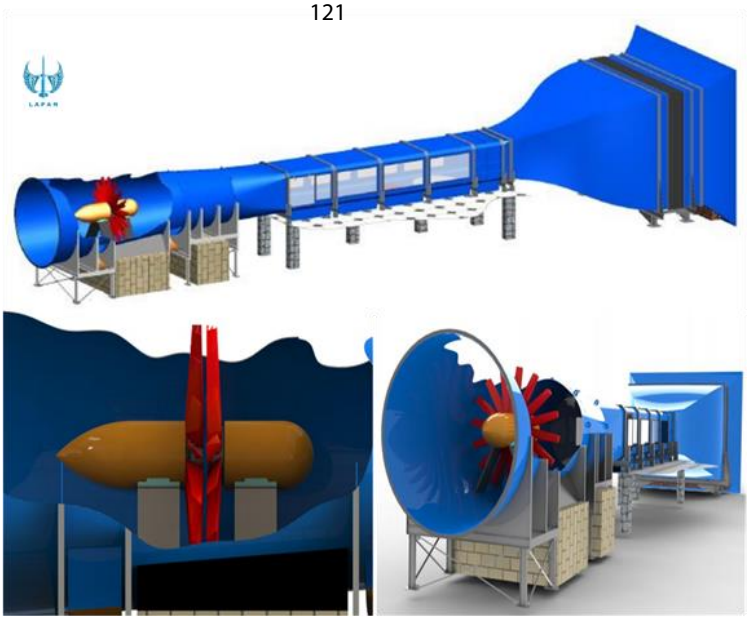

Figure 2-7. LAPAN low-speed tunnel (LLST).

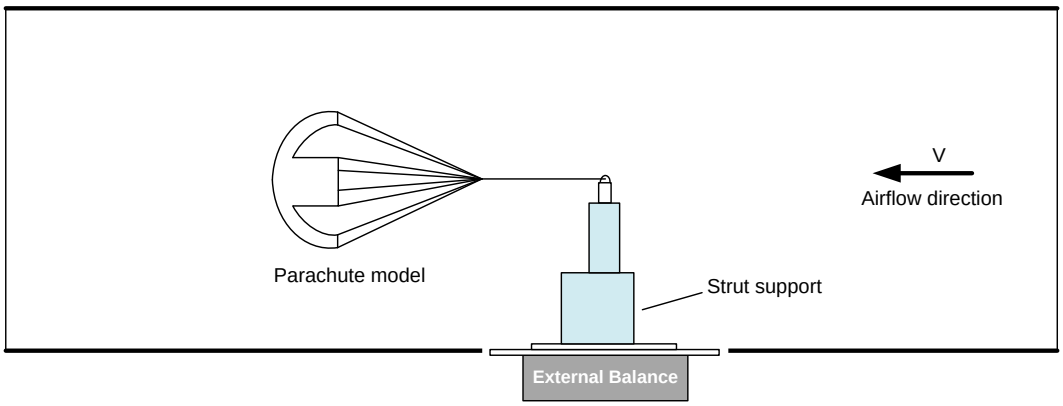

Figure 2-8. Schematic drawing of model installation for aerodynamic force measurement by using external balance.

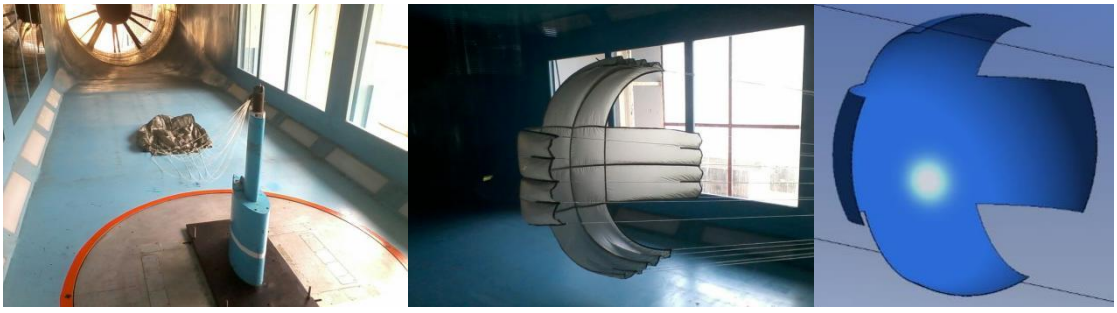

Figure 2-9. Model of the parachute at Wind tunnel test and simulation. (Herdiana, 2014)

3. Result and Analysis

Results of the simulation and the wind tunnel test are presented in the graphical format which are shown in Figure 3-13-1 until Figure 3-.

3.1. Results of the simulation and the wind tunnel test

The drag is counted when velocity and force are stabilized. For wind tunnel results, the drag coefficient of the model varies from 1.504 to 2.12 at 10 m/s, and for simulation results, the drag coefficient of the model from 2.21 to 2.22 at 10 m/s as shown in Figure 3-1. From 6 m/s the drag coefficient gradient is small and almost flat in an area of 2.

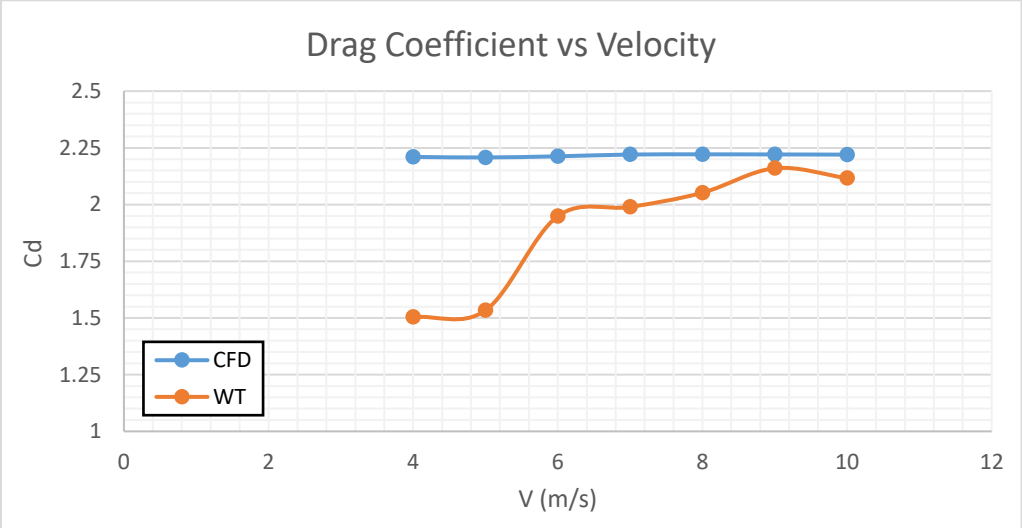

Figure 3-1. Drag coefficient of parachute for various velocities.

The graph for the drag force versus velocity is shown in the trend of the drag curve is shown correctly, the force increases with increasing velocity. At a maximum velocity of 10 m/s, the drag force value is 10.38 kg. f and the drag coefficient is 2.12. So the average drag coefficient from wind tunnel results is 1.9. In the graph, it can be seen that the velocities of 4 m/s and 5 m/s experienced differences because, during the testing process, the parachute was still in a vibrating/shaking condition so the data collection was less than perfect. After all, the parachute model was vibrating/shaking. Test data collection is carried out only once.

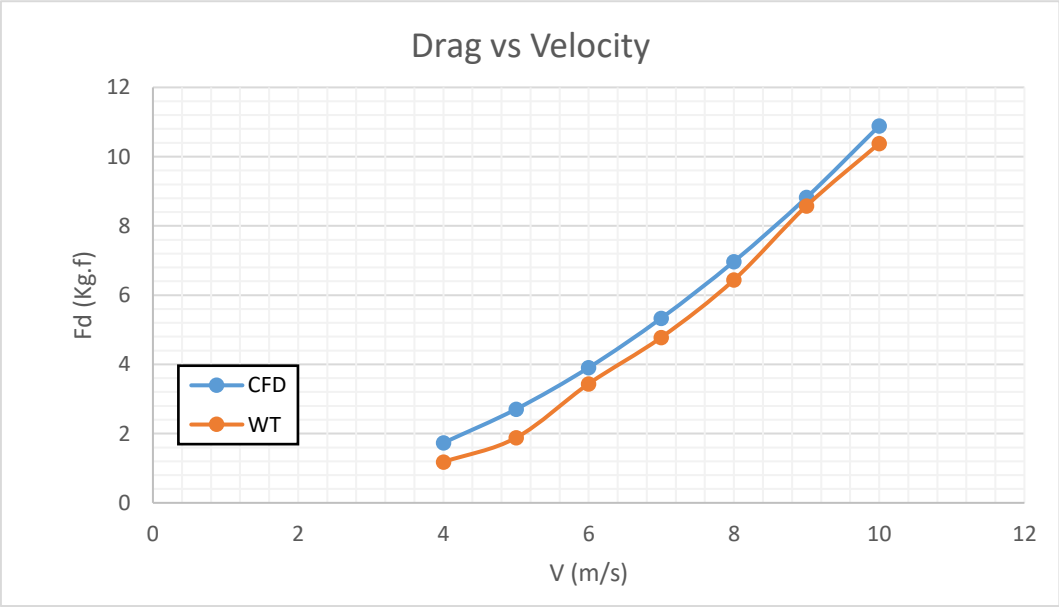

Figure 3-2. Drag force of parachute for various velocities.

Figure 3-2 shows a comparison of the results of the simulation and testing in the wind tunnel on changes in velocity. The graph shows the same trend but the drag force from the simulation results is greater than the test results. The average difference between the simulation results and wind tunnel testing is around 18%. The greater the velocity of descent on the parachute, the greater the drag force generated with the fixed canopy diameter.

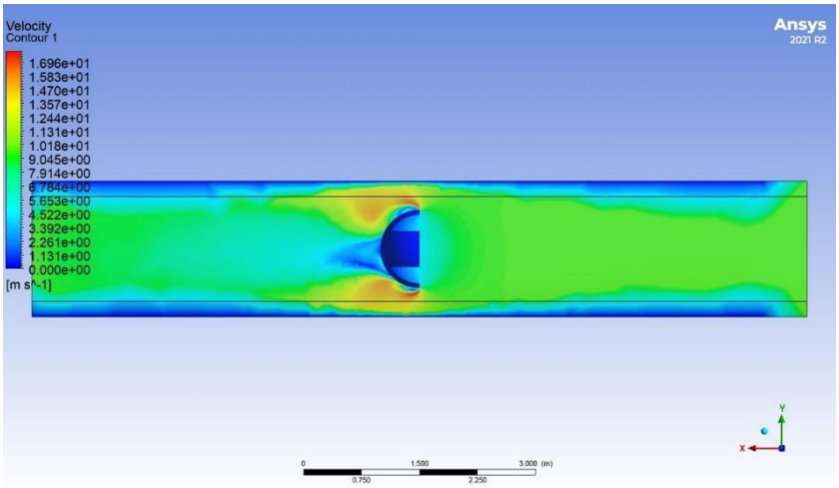

Figure 3-3. Flow visualization in simulation at 10 m/s (ANSYS, 2023).

Figure 3-3 shows the flow visualization of the simulation results. In the figure shows the change in velocity of the parachute in a wind tunnel, the orange color shows the velocity is higher than the setup velocity which is 10 m/s.

3.2. Parachute comparison

A comparison of the different types of parachutes was intended to check the different drag at the same velocity and diameter canopy. Two types of parachutes are compared, which are the hemisphere/annular type and the cross/cruciform type.

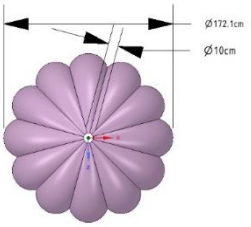

V (m/s)	D (m)	A (m^2)	Fd
2	2.15	3.64	19.62
2.5	1.72	2.33	19.62
3	1.44	1.62	19.62
3.5	1.23	1.19	19.62
4	1.08	0.91	19.62

Analytic results of hemisphere/annular type (Dana Herdiana, 2023)

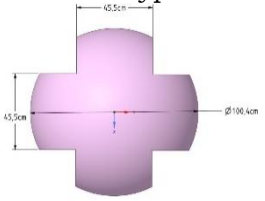

V (m/s)	Fd (N)
4	17.01
5	26.55
6	38.32
7	52.34
8	68.39
9	86.54
10	106.80

Results of cross/cruciform type

Figure 3-4. Comparison between different types of parachutes.

In comparing the two types of parachutes (figure 3-4), it can be seen that the canopy diameter and descent velocity are the same. Canopy diameter of about 1 m and descent velocity of 4 m/s. In the comparison between hemisphere and cross-type for simulation results, there is a difference in drag at the descent velocity of 4 m/s. The cross-type has a smaller drag force than the hemisphere type, the difference is around 2.61 N (0.266 kg. f).

Simulation result of canopy design

Parachute design	Annular canopy			Cruciform canopy		
	A_1	B_1	C_1	A_2	B_2	C_2
C_d	0.7875	0.7915	0.8039	0.7836	0.7855	0.7970

Figure 3-5. Compare the drag coefficient of the annular and cruciform canopy (Raudah Saim, 2020).

Figure 3-5 shows the results of the simulation carried out by the Raudah team (Raudah Saim, 2020) with different parachutes and different numbers of grids. A1, B1, C1, A2, B2, and C2 are the unstructured grids around the canopy design.

3.3. Rope length contribution

The testing found that rope length contributed to the change of drag. From Figure 3-3-6, it can be seen that shorter rope lengths contribute to the reduction of drag value. This reduction is caused by the shorter rope makes the diameter canopy of the parachute smaller than the long lines. In total, the average reduction of drag force by making the rope shorter is about 0.5 kg. f. With this result, the length of rope lines would be changed.

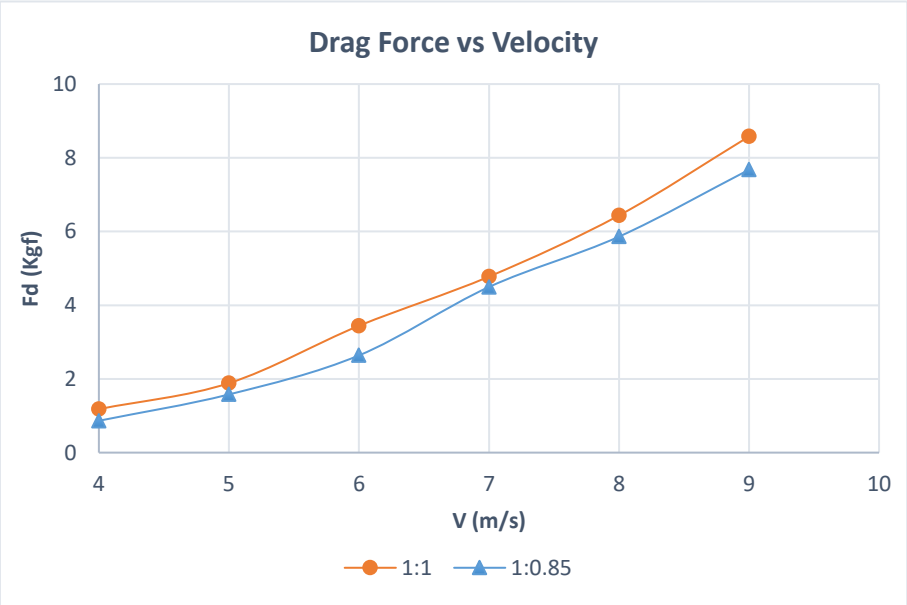

Figure 3-6. Drag force comparison for different rope lengths.

By taking the average drag coefficient value for the parachute model from the wind tunnel test result is around 1.9, it produces the descent velocity for the aircraft of 1.72 m/s. So the parachute design for this aircraft is slightly larger than the target of 6 m canopy diameter. This value is not far from the target of 2 m/s. Therefore, this initial parachute design value can be used as the recovery system of a 10 kg class UAV.

4. Conclusions

From the simulation and testing, the following conclusion can be taken:

- The initial design value is to fulfill the target design. Therefore, the parachute is feasible to be used as a UAV recovery system
- Detail calculation or testing to determine aircraft drag in vertical components shall be conducted to get an accurate result.
- Validation by means of a drop test shall be performed.
- The cross shape has a smaller drag force than the hemisphere shape at the same descending velocity of 4 m/s.
- The descent velocity for the aircraft is smaller than the target.
- The parachute design for the aircraft is slightly larger than the target.

Acknowledgments

This study was facilitated by LAPAN (BRIN) and Dislitbang AU. Also to the technician team who supported the testing process, and Mr. Agus Aribowo who guided the research process.

Contributorship Statement

A not sole author manuscript must write their contribution statement. The contribution statement may be written in detail as follows (Note: the author's initials are

DH, TMIH, AMP, and W): DH developed the experiments and designed the method, TMIH analyzed the results and prepared the manuscript, AMP prepared the manuscript, and W prepare the wind tunnel test.

The contribution statement may also be written as follows: DH, TMIH, and AMP are the main contributors.

Statement Of Author

All Authors in this paper and research are Main Contributors.

References

ANSYS. (2023). *Software Package, V 21.0.*

Dana Herdiana, A. R. (2023). Parachute Design for Payload on LSU02 VTOL Aircraft. *AIP Conference Proceedings 2592 ICOMEET 2021, https://doi.org/10.1063/5.0115922.* AIP Publishing.

Gamiz, U. F. (2013). *Fluid Dynamic Characterization of Vortex Generator and Two-dimensional Turbulent Wakes.* Catalonia: A Thesis for Doctor of Philosophy, Polytechnic University of Catalonia (UPC).

Herdiana, D. (2014). *Model Parachute Recovery System Type Cross Testing at LAPAN Subsonic Wind Tunnel.* LAPAN.

Hoerner, S. F. (1965). *Fluid-Dynamic Drag.* Brick Town, New Jersey 08723.

Hou Xia-yi, H. J. (2022). Numerical study on ring slot parachute finite mass inflation process and wake recontact phenomenon. *Aerospace Science and Technology 128*.

J S. Lingard, A. S. (2017). Supersonic Parachute Testing Using a MAXUS Sounding Rocket Piggy-Back Payload. *24th AIAA Aerodynamic Decelerator Systems Technology Conference.* Denver, Colorado: The American Institute of Aeronautics and Astronautics, Inc., with permission.

Keith Stein, R. B. (1999). Fluid-Structure Interaction Simulation of a Cross Parachute: Comparison of Numerical Predictions With Wind Tunnel Data. *AIAA Paper 99-1725, Proceedings of the 15th CEAS/AIAA Aerodynamic Decelerator Systems Technology Conference and Seminar.* Toulouse, France: AIAA.

Keith Stein, R. B. (2001). Fluid-structure Interaction of a Cross Parachute: Numerical Simulation. *Computer Methods Applied Mechanics and Engineering, Elsevier*, 673-687.

Knacke, T. W. (t.thn.). *Parachute Recovery Systems Design Parachute Recovery Systems Design.* Santa Barbara, CA: Distributed by Para-Publishing.

L. Pepermans, T. B. (2021). Architectures for Parachute Testing. *IAC 2021*. Dubai: IAF.

NASA. (t.thn.). *Shape Effect On Drag*. Dipetik October 2015, dari http://www.grc.nasa.gov/WWW/k-12/airplane/shaped.html

Nimesh Dahal, K. F. (2020). Classification of Supersonic Flow Over a Rigid Parachute Model With Suspension Lines. *Aerospace Science and Technology, 105*.

Pustekbang LAPAN. (t.thn.). *LAPAN Surveillance UAV 02*. Dipetik October 29, 2015, dari www.lapan.go.id

Raudah Saim, S. M. (2020). Computational Fluid Dynamic (CFD) Analysis of Parachute Canopies Design for Aludra SR-10 UAV as a Parachute Recovery Systems (PRS). *CFD Letters, www.akademiabaru.com/cfdl.html*, 46-57.

S. Steinberg, P. S. (1974). Development of the Viking Parachute Configuration by Wind-Tunnel Investigation. *Journal Spacecr. Rocket, 11*, 101 - 107.

Smagorinsky, J. (1963). General Circulation experiments with the primitive equations. *Monthly Weather Review 91*, hal. 99-165.

T.E. Tezduyar, S. A. (1994). Massively parallel finite element simulation of compressible and incompressible flows. *Computer Methods Applied Mechanics and Engineering, 119*, 157-177.

Wang Xufeng, K. X. (2015). Real-time drogue recognition and 3D locating for UAV autonomous aerial refueling based on monocular machine vision. *Chinese Journal of Aeronautics, 28*(6), 1667-1675.

Xiao-peng Xue, H. K.-Y. (2015). Effects of suspension line on flow field around a supersonic parachute. *Aerospace Science and Technology vol. 43, In Press*, 63-70.

Xiaopeng Xuea, Y. N.-Y. (2017). Numerical Investigation of Effects of Angle-of-Attack on a Parachute-like Two-body System. *Aerospace Science and Technology*(http://dx.doi.org/10.1016/j.ast.2017.06.038).

Zhibin Li, W. C. (2021). An Estimation Method for Parachute Parameters. *Journal of*

Physics: Conference Series 1786.